

Synthesis of hexadecylamine capped nanoparticles using group 12 complexes of N-alkyl-N-phenyl dithiocarbamate as single-source precursors

Peter A. Ajibade^{a,*}, Damian C. Onwudiwe^a, Makwena J. Moloto^b

^a Department of Chemistry, University of Fort Hare, Private Bag X1314, Alice, South Africa

^b Department of Chemical Technology, University of Johannesburg, P.O. Box 17011, Doornfontein 2028, South Africa

ARTICLE INFO

Article history:

Received 12 August 2010

Accepted 19 October 2010

Available online 9 November 2010

Keywords:

Metal complex

Dithiocarbamates

HgS

CdS and ZnS nanoparticles

Precursors

ABSTRACT

Metal complexes of the type ML^1L^2 [$M = Zn, Cd, Hg$; $L^1 = N$ -methyl- N -phenyldithiocarbamate and $L^2 = N$ -ethyl- N -phenyldithiocarbamate] have been synthesized and characterized by elemental analyses, FT-IR and NMR spectroscopy. The complexes are formulated as four coordinate species with the dithiocarbamates acting as bidentate chelating ligands. The complexes were thermolysed and used as single-source precursors for the synthesis of HDA-capped MS ($M = Zn, Cd, Hg$) nanoparticles. The HgS nanoparticles show a narrow size distribution from their TEM images, while the CdS nanoparticles gave crystalline particles with a sharp band absorption edge and a narrow PL band. The ZnS nanoparticles gave crystalline particles with a stacking arrangement.

© 2010 Elsevier Ltd. All rights reserved.

1. Introduction

Coordination compounds containing ligands with sulfur atoms as donors have received much attention [1]. Among these sulfur containing ligands, the dithiocarbamate species ($RR'NCS^-$) form an important family of classical anionic ligands [2] and are very relevant to the chemistry of disulfides. These anions, derived from secondary amines, are versatile chelating agents. The strong chelating property is utilized in their extensive use as separating agents in gas chromatography [3] and liquid–liquid extraction [4], in purification [5], as fungicides in agriculture [6] and antidotes to fight metal poisoning [7]. The anions are three-electron donors [8] and have a small bite angle (~ 2.8 – 2.9 Å) [9]. Hence, they are able to delocalize the positive charge from the metal toward the periphery of the complex and this stabilizes the metal ions [8,10]. These ligands, apart from their vast technological applications, are of interest as a potential source of novel structures [11]. Dithiocarbamate complexes of group 12 represent a large and interesting class of inorganic compounds [12] and they have been widely studied in recent years. Some of the studies of these d^{10} complexes have been made to understand the interactions which exist between the metal ion and the ligands [11], and for their use as single-source precursors for semiconductor nanoparticles.

The use of single-source molecular precursors in which a metal–chalcogenide bond is available has proven to be a very efficient

* Corresponding author. Tel.: +27 40 602 2055; fax: +27 40 6022094.

E-mail address: pajibade@ufh.ac.za (P.A. Ajibade).

route to high-quality nanoparticles [13]. Since the introduction of a single source precursor as an alternative and most convenient approach to the synthesis of semiconductor nanoparticles, the compounds that have found the greatest dissemination as precursors for II–VI semiconductors are the dithiocarbamate complexes [14]. Dialkyldithiocarbamate complexes [$M(S_2CNR_2)_2$] ($M = Zn(II), Cd(II), R = alkyl$) have been used as single-source precursors to prepare nanoparticles and to deposit ZnS or CdS thin films by metal–organic chemical vapour deposition (MOCVD) [15]. O'Brien et al. have developed a series of Zn and Cd complexes of dithiocarbamates as precursors to prepare II–VI chalcogenides which yielded high-quality nanocrystals organically capped with tri- n -octylphosphine oxide (TOPO) [16–18], and also carried out in depth studies on the effect of side groups on the deposition temperature and decomposition mechanisms [19]. Asymmetrical four coordinate dithiocarbamates $M(E_2CNR^1R^2)_2$ have proved relatively better than the symmetrical dithiocarbamates for the synthesis of nanoparticles and growth of chalcogenide films because they are sufficiently more volatile. Hence, the relative use of dithiocarbamates as single-source precursors depends on both the nature of the alkyl substituent and the dithiocarbamate groups. There are relatively few reports on dithiocarbamates as a single source precursor for mercury chalcogenides. Green et al. [20] have reported the synthesis of mercury (II) N,N' -methyl-phenyl ethyl dithiocarbamates and their use as a precursor for the room temperature deposition of a HgS thin film. In this paper we report the synthesis and characterization of some N-alkyl-N-phenyl dithiocarbamate complexes of Zn(II), Cd(II) and Hg(II) and their use as single molecular precursors for nanoparticles.

2. Experimental

2.1. Chemicals

Hexadecylamine (HDA) and triⁿoctylphosphine (TOP), toluene and absolute methanol were purchased from Aldrich. Toluene was dry and stored over molecular sieves (4.0 Å) before use. All other solvents and metal salts were of analytical grade obtained from Aldrich and were used without further purification. The ligands sodium *N*-methyl-*N*-phenyldithiocarbamate and sodium *N*-ethyl-*N*-phenyl dithiocarbamate were prepared by a modified procedure given in the literature [21].

2.2. Physical measurements

Infrared spectra were recorded from KBr pellets in the range 4000–400 cm⁻¹ on a Perkin–Elmer 2000 FT-IR spectrometer. NMR spectra were recorded on a Bruker NMR spectrometer (400.1 MHz for ¹H, 100.6 MHz for ¹³C). Microanalysis was carried out on a Fisons elemental analyzer. The optical measurements were carried out using an Analytikjena Specord 50 UV–Vis spectrophotometer. The samples were placed in glass cuvettes (1 cm path length) using toluene and methanol as a reference solvents for the nanoparticles. A Perkin–Elmer LS 45 Fluorimeter was used to measure the photoluminescence of the nanoparticles by dissolving them in toluene and placing the samples in glass cuvettes (1 cm path length) for analysis. The X-ray diffraction patterns were recorded by a Phillip's X'Pert materials research diffractometer at 40 kV/50 mA using secondary graphite monochromated Cu K α radiation ($\lambda = 1.5406$ Å). Measurements were taken at a high angle 2θ range of 20–90° with a scan speed of 0.01°. The TEM images were obtained using a Philips CM 200 compustage electron microscope operated at 200 kV. The samples were prepared by placing a drop of a dilute solution of the sample in toluene on a copper grid (400 mesh, agar).

2.3. Synthesis of the complexes

The same synthetic procedure was used for all the complexes: a solution of sodium *N*-methyl-*N*-phenyldithiocarbamate, **L**¹ (0.256 g, 1.25 mmol) and sodium *N*-ethyl-*N*-phenyldithiocarbamate, **L**² (0.274 g, 1.25 mmol) in 20 mL of water at room temperature was added to (1.25 mmol) Zn(OOCCH₃)₂·2H₂O (0.274 g), CdCl₂·2.5H₂O (0.230), HgCl₂ (0.340) in 20 mL of water to obtain an immediate precipitation. After stirring for 1 h, the precipitate was filtered off, rinsed thoroughly with water and dried *in vacuo*.

2.3.1. ZnL¹L²

The complex was obtained as a white solid. Yield: 0.435 g, (78.52%), m.p. 212–214 °C. ¹H NMR (CDCl₃) $\delta = 7.44$ – 7.34 (m, C₆H₅–N(Et)), 7.30– 7.22 (m, C₆H₅–N(Me)), 4.18 (q, CH₂–N(Et)), 1.53 (s, CH₃–N(Me)), 1.28 (t, CH₃–(Et)). ¹³C NMR (CDCl₃) $\delta = 207.29$, 206.44 (CS₂), 146.10, 144.07 (C₆H₅–N(Et)), 129.61, 128.65, 128.56, 126.70 (C₆H₅–N(Me)), 53.97 (CH₂–(Et)), 46.89 (CH₃–N(Me)), 12.38 (CH₃–(Et)). Selected IR, $\nu(\text{cm}^{-1})$: 1458 (C=N), 1276 (C₂–N), 939 (C=S). *Anal. Calc.* for C₁₇H₁₈N₂S₄Zn (443.96): C, 45.99; H, 4.09; N, 6.31; S, 28.89. *Found:* C, 46.33; H, 4.19; N, 6.32; S, 28.92%.

2.3.2. CdL¹L²

The complex was obtained as a white solid. Yield: 0.48 g (78.37%), m.p. 248–250 °C. ¹H NMR (CDCl₃) $\delta = 7.43$ – 7.38 (m, C₆H₅–N(Et)), 7.31– 7.22 (m, C₆H₅–N(Me)), 4.12 (t, CH₂–N(Et)), 1.15 (t, CH₃–(Et)). ¹³C NMR (CDCl₃) $\delta = 208.27$, 207.55 (CS₂), 148.10, 146.00 (C₆H₅–N(Et)), 129.15, 127.57, 126.84, 125.80

(C₆H₅–N(Me)), 54.67 (CH₂–(Et)), 46.26 (CH₃–N(Me)), 12.09 (CH₃–(Et)). Selected IR, $\nu(\text{cm}^{-1})$: 1456 (C=N), 1278 (C₂–N), 939 (C=S). *Anal. Calc.* for C₁₇H₁₈N₂S₄Cd (490.99): C, 41.59; H, 3.70; N, 5.71; S, 26.12. *Found:* C, 42.01; H, 3.92; N, 5.79; S, 26.09%.

2.3.3. HgL¹L²

The complex was obtained as a greenish ash colour. Yield: 0.520 g, (72%), m.p. 218 °C. ¹H NMR (CDCl₃) $\delta = 7.42$ – 7.33 (m, C₆H₅–N(Et)), 7.28– 7.24 (m, C₆H₅–N(Me)), 4.16 (q, CH₂–N(Et)), 1.53 (s, CH₃–N(Me)), 1.26 (t, CH₃–(Et)). ¹³C NMR (CDCl₃) $\delta = 206.43$, 205.84 (CS₂), 147.47, 145.26 (C₆H₅–N(Et)), 129.66, 128.80, 126.43, 125.34 (C₆H₅–N(Me)), 55.86 (CH₂–(Et)), 48.93 (CH₃–N(Me)), 12.26 (CH₃–(Et)). Selected IR, $\nu(\text{cm}^{-1})$: 1459 (C=N), 1280 (C₂–N), 966 (C=S). *Anal. Calc.* for C₁₇H₁₈N₂S₄Hg (579.17): C, 35.25; H, 3.13; N, 4.84; S, 22.14. *Found:* C, 35.39; H, 3.24; N, 4.68; S, 21.96%.

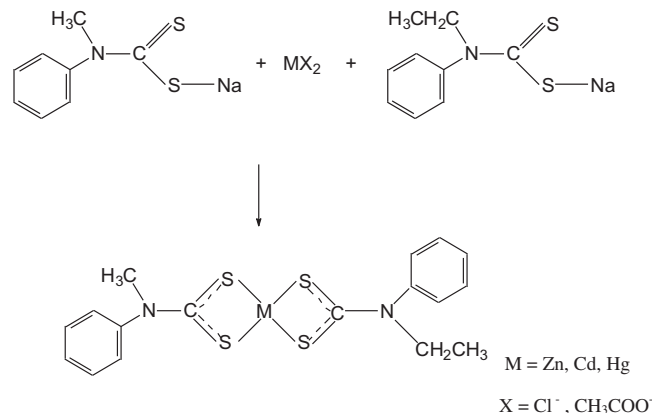
2.4. Synthesis of HDA-capped nanoparticles

The metal sulfide nanoparticles were prepared from their respective metal complexes. In a typical synthesis, the metal complexes (0.50 g) were each dissolved in TOP (10 mL) and injected into hot HDA (7 g) at 120 °C. An initial decrease in temperature (by about 20–30 °C) was observed. The solution was stabilized and the reaction was continued for 1 h at 120 °C. After completion, the reaction mixture was allowed to cool to 70 °C and methanol was added to precipitate the nanoparticles. The solid was separated by centrifugation and washed three times with methanol. The resulting solid precipitates of HDA-capped MS nanoparticles were dispersed in toluene for further analysis.

3. Results and discussion

3.1. Synthesis

Sodium salts of the ligands were obtained by the reaction of the secondary amines with CS₂ and sodium hydroxide in aqueous medium at low temperature. The white solids obtained were stable at room temperature. The metal complexes were conveniently obtained in high yield at room temperature by the substitution reaction of NaL¹, NaL² and the respective metal salts in equimolar ratios in water, following Scheme 1. These complexes are air-stable and the Zn(II) and Hg(II) complexes are soluble in dichloromethane and chloroform. The poor solubility of the cadmium complex in both organic and inorganic solvents could be attributed to the possibility of the complex existing in the polymeric form. The



Scheme 1. The preparation of *N,N*-methyl phenyl-*N,N*-ethyl phenyl dithiocarbamate complexes.

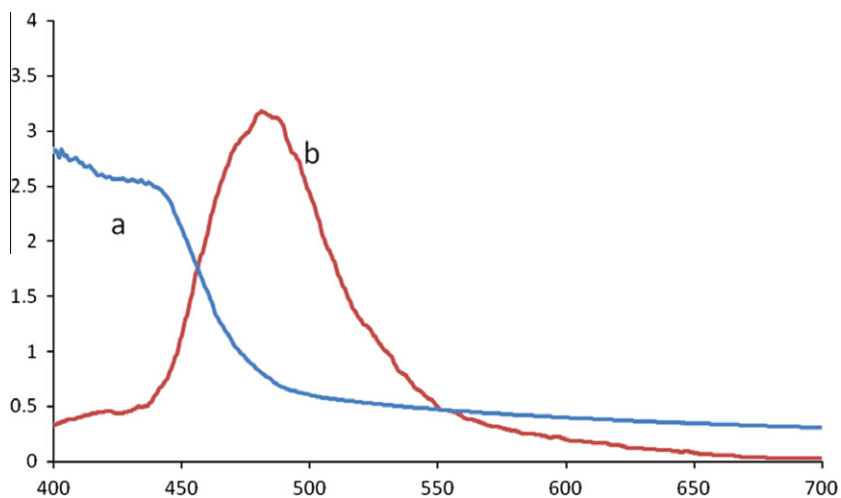


Fig. 1. Absorption (a) and emission (b) spectra of HDA-capped CdS nanoparticles prepared from the cadmium complex.

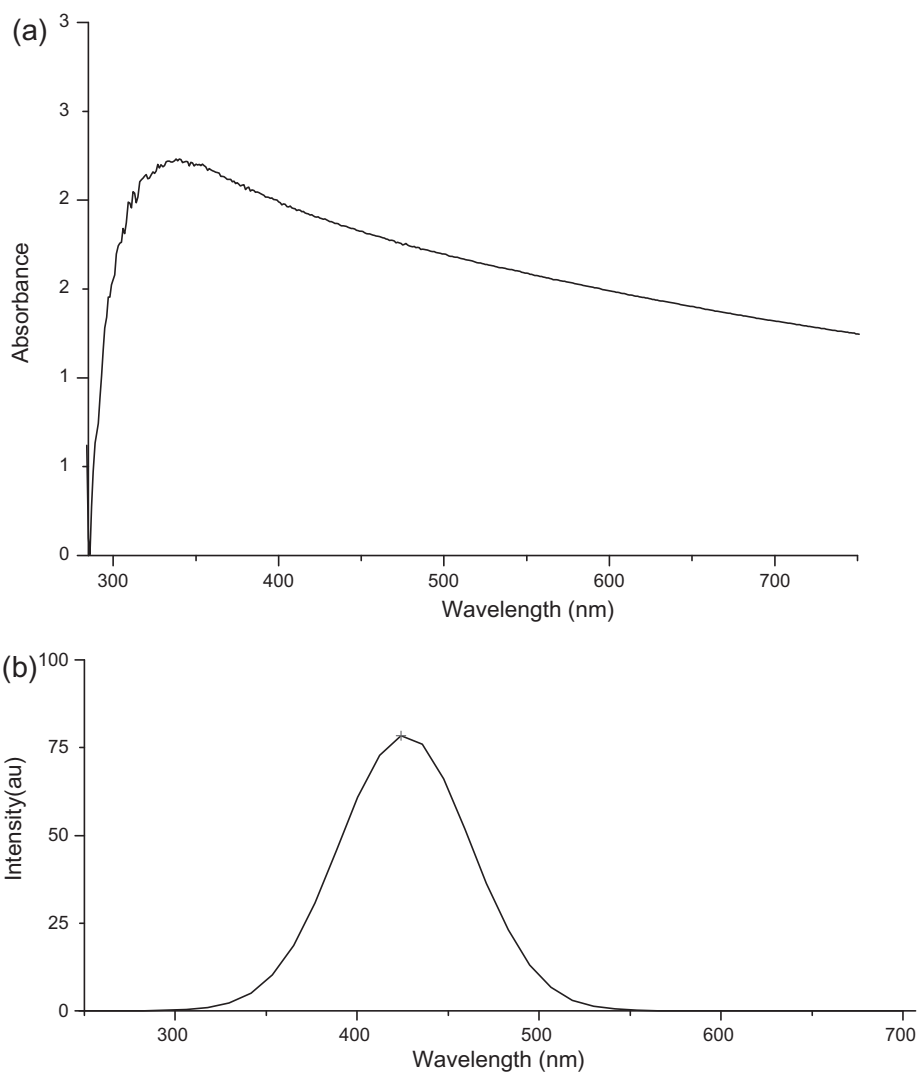


Fig. 2. Absorption (a) and emission (b) spectra of HDA-capped HgS nanoparticles prepared from the mercury complex.

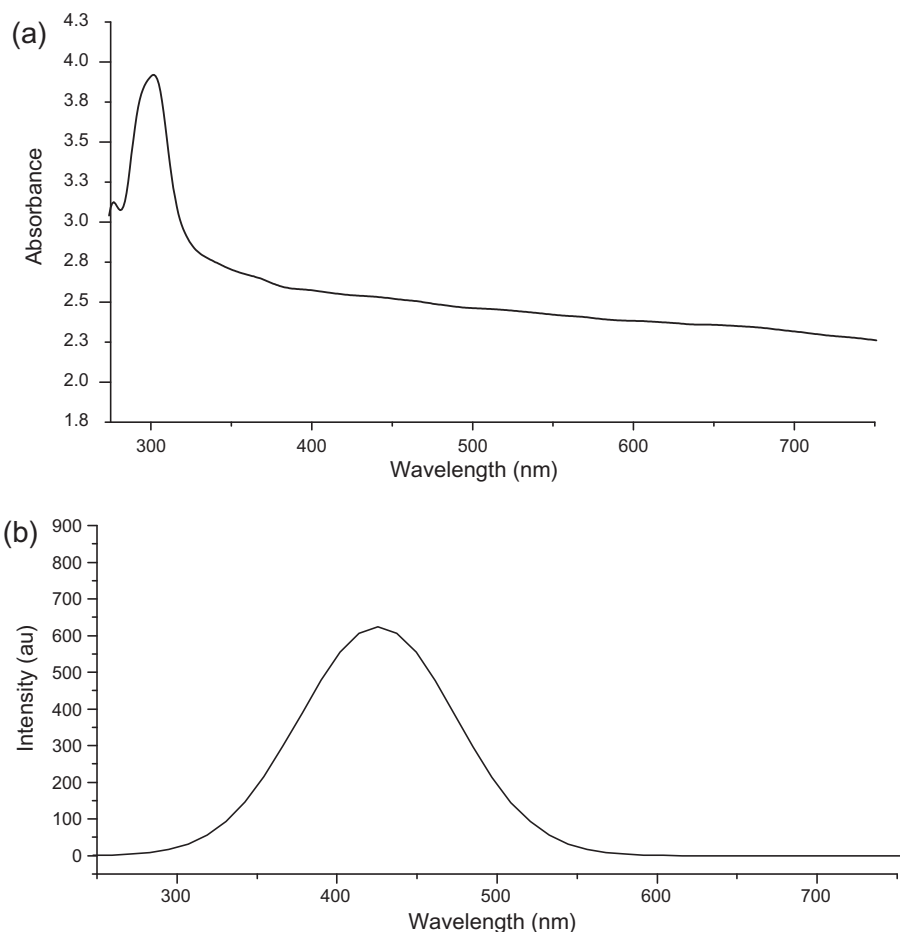


Fig. 3. Absorption (a) and emission (b) spectra of HDA-capped ZnS nanoparticles prepared from the zinc complex.

formation of polymers might be due to the fact that dithioacard complexes of the ML_2 type are coordinatively unsaturated, thus leading to the formation of a higher coordination number either by the addition of one or two molecules of a Lewis base or by polymerization of ML_2 [22].

3.2. Infrared spectral studies

Infrared spectra of the ligands and the complexes were compared and assigned on careful comparison. In both ligands, the strong peaks were observed around 3335 and 3174 cm^{-1} due to symmetrical and asymmetrical $\nu(\text{O-H})$ vibrations of water molecules in the sodium salt of the dithiocarbamates [23]. These peaks were completely absent in all the complexes, indicating the loss of the water molecules upon coordination to the metal ions. An observed feature of the spectra of the three compounds is the CN bond observed at 1458 , 1458 and 1459 cm^{-1} for the Zn, Cd and Hg complexes, respectively. These $\nu(\text{C-N})$ bands are shifted to higher energy relative to the ligands (*ca.* 1453 cm^{-1}). The shift is a reflection of increased bond strength. This strengthening of the CN bond is ascribed to the increase in the double bond character, which is observed upon coordination to the metal centre [24,25]. The difference in the electron releasing ability of the organic groups affects the electron density on the sulfur atom *via* the π -system and therefore influences the double bond character of the C=N bond [24]. These peaks observed for the complexes fall within the stretching frequencies of $\nu(\text{C-N})$ 1250 – 1350 cm^{-1} and $\nu(\text{C=N})$ 1640 – 1690 cm^{-1} [26]. The close similarities in the positions of the bands strongly suggest similar coordination modes

for the complexes. An established criterion for the bonding modes in dithiocarbamates uses the number of bands observed in the region $1000 \pm 50\text{ cm}^{-1}$ to determine the coordination mode of the dithiocarbamate ligand to the metal ion [27,28]. In the above region, a single sharp band implies a symmetrical bidentate coordination, while the splitting of this band into a doublet may indicate a monodentate unsymmetrical coordination of the dithiocarbamate group. All the compounds show a single peak within this region which implies the presence of symmetrically bonded bidentate dithiocarbamates. Peaks in the region 2930 – 2960 cm^{-1} can be assigned to $\nu(\text{C-H})$ of the alkyl groups. The $\nu(\text{M-S})$ peaks are characteristically found in the far infrared region, typically between 300 and 400 cm^{-1} . This peak usually depends on the nature of the organic substituent attached to the nitrogen atom [29].

3.3. ^1H and ^{13}C NMR

In the ^1H NMR spectra, all the chemical shifts were found in the expected regions, only subtle differences were observed from one complex to another. The electronic and magnetic influence of the alkyl substituent's ($-\text{CH}_3$ and $-\text{C}_2\text{H}_5$) are evidenced in the resonance spectra observed in the upfield region. All the spectra contain a set of quartets around 4.15 ppm, assigned to the methylene protons, and a sharp singlet at about 1.53 ppm, associated with the methyl group bound to an electronegative nitrogen atom. This peak is differentiated from the $-\text{CH}_3$ of the ethyl substituent, which was observed around 1.20 ppm, since the magnitude of the deshielding decreases with the increase in distance from the metal centre or the thioureide bond [30]. The protons of the

aromatic unit appear in two groups as complex multiplets between 7.44 and 7.22 ppm.

The ^{13}C NMR spectra of all the compounds exhibit a low field resonance associated with the backbone carbon of the dithiocarbamate [31]. Two distinct peaks were observed at *ca.* 207.00 and 206.00 ppm. Each of these signals is said to indicate the contribution of the double bond character to a formally single N–C bond in the dithiocarbamate group, i.e., the admixture of the sp^2 hybridized state to the sp^3 orbitals of the nitrogen atom, thus a considerable δ^+ surplus charge is localized on the nitrogen atom, while a δ^- charge is delocalized through the four-membered metallochelate ring – CS_2M [32]. The occurrence of two NCS_2 peaks is attributed to the influence of the different organic substituents on their magnetic equivalence. The ligating group (dithiocarbamate) with the greater electronic density has a more shielded $-\text{CS}_2$ carbon [33]. The methylene carbon of the ethyl group resonates around 54.00 ppm, while the N– CH_3 appears at around 47.00 ppm. It experiences a more deshielding effect than the $-\text{CH}_3$ of the ethyl group, which resonates around 12.20 ppm, due to the influence of the electronegative nitrogen and the thioureide π -system [30,34]. In the aromatic region, two sets of signals were observed; two peaks of low intensity between 148.00 and 144.00 ppm, which are assigned to the aromatic carbons of the N-ethyl unit. The second set of aromatic peak occurred as four peaks of relatively high intensity between 129.00 and 125.00 ppm, which is due to the N-methyl unit. The occurrence of these peaks in different environments indicates the magnetic unequivalence of the aromatic groups [35].

3.4. Synthesis and characterization of nanoparticles

The complexes of mercury, cadmium and zinc used for the nanoparticles synthesis were synthesized from aqueous media at room temperature. The complexes crystallize into yellow to white precipitates in relatively good yields. Variation of the alkyl groups on the dithiocarbamate ligand always gave particles with non-spherical morphologies [36,37], and in this work a mixture of short alkyl and phenyl groups are investigated for their effect on the nature of the particles produced. A lot of factors contribute towards the sizes and shapes of particles, and hence influence the absorption and emission features. Therefore the optical and morphological properties will be discussed next.

3.4.1. Optical properties of CdS, HgS and ZnS nanoparticles

All the semiconductor nanoparticles CdS, HgS and ZnS, prepared from their respective complexes, showed a blue shift in their absorption band edges (Figs. 1–3). CdS (469 nm and emission at 484 nm – λ_{exc} at 450 nm), HgS (excitonic feature at 335 nm with typical tailing of the absorption band and emission maximum at 425 nm) and ZnS nanoparticles (with an excitonic feature at 337 nm tailing and emission maximum at 424 nm). The tailing of the absorption features from ZnS and HgS results from the particle sizes ranging from significantly small to larger and growth of particles in the form of layers of concentric circles. CdS nanoparticles showed a sharp band edge, and narrow emission bands were observed for CdS and HgS nanoparticles with the width typical of small particles size range and that of ZnS gave a wider band gap of about 320 nm. All gave emission maxima which are red shifted to the absorption band edges, ranging from 21 to 79 nm. CdS nanoparticles from heterocyclic dithiocarbamate complexes were reported to produce rods, tripods and tetrapods, depending on the concentration and temperature [34,35] with absorption features similar to the CdS nanoparticles obtained in this work.

3.4.2. Structural characterization of CdS, HgS and ZnS nanoparticles

Generally, complexes such as cadmium, mercury and zinc with the ligand alkylphenyldithiocarbamate produce metal sulfides due

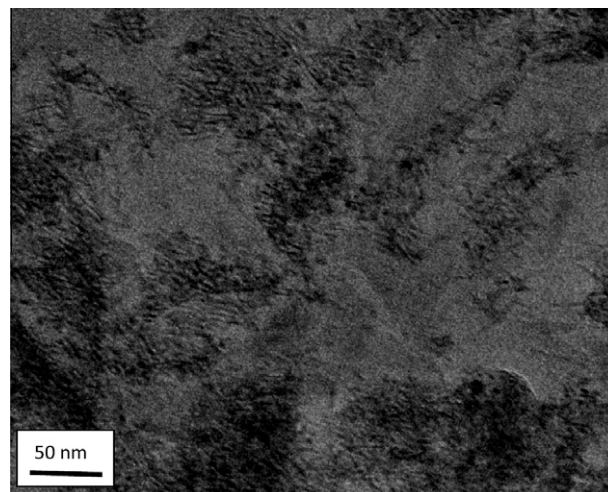


Fig. 4. TEM image of HDA-capped CdS nanoparticles from the cadmium complex.

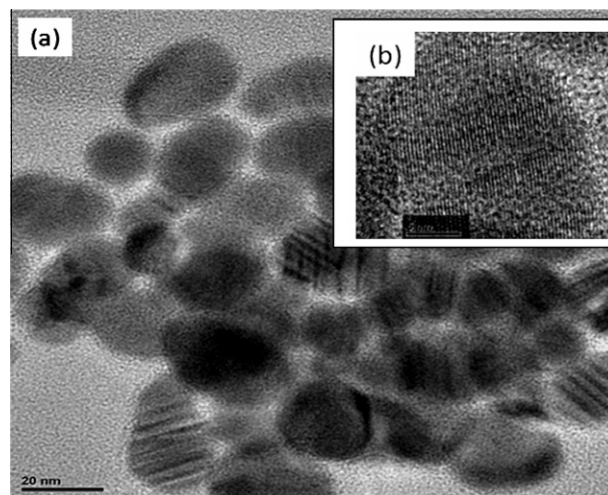


Fig. 5. TEM image of HDA-capped HgS nanoparticles (a) from its corresponding complex with HRTEM images for the spherical particles (b).

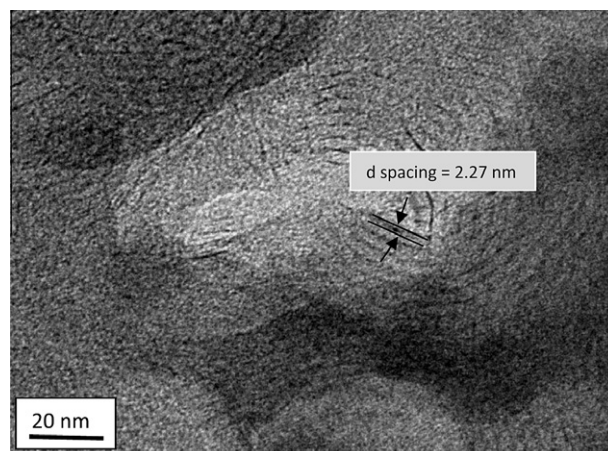


Fig. 6. TEM image of HDA-capped ZnS nanoparticles from its corresponding complex.

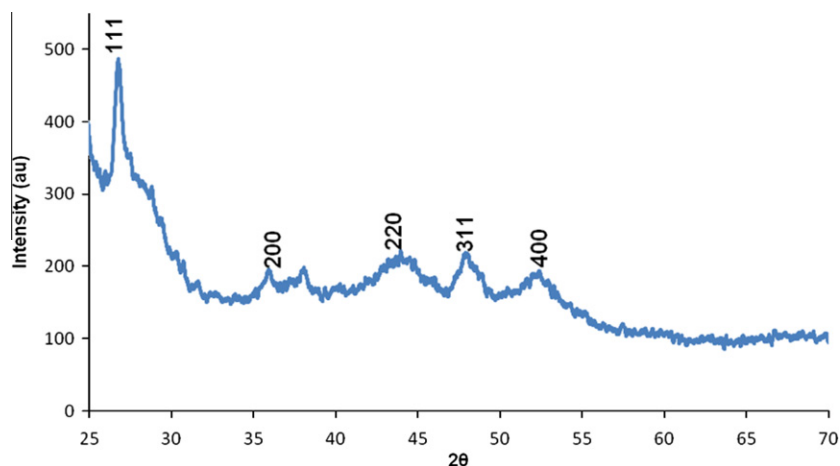


Fig. 7. XRD patterns of HDA-capped CdS nanoparticles prepared from its complex.

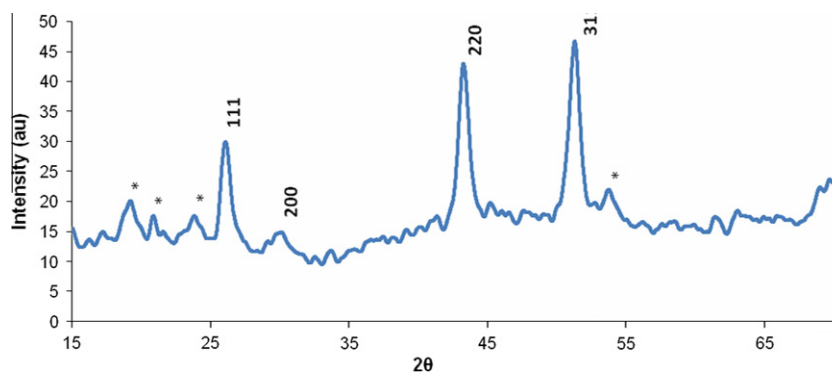


Fig. 8. XRD patterns of HDA-capped HgS nanoparticles prepared from its complex (* – peaks due to HDA).

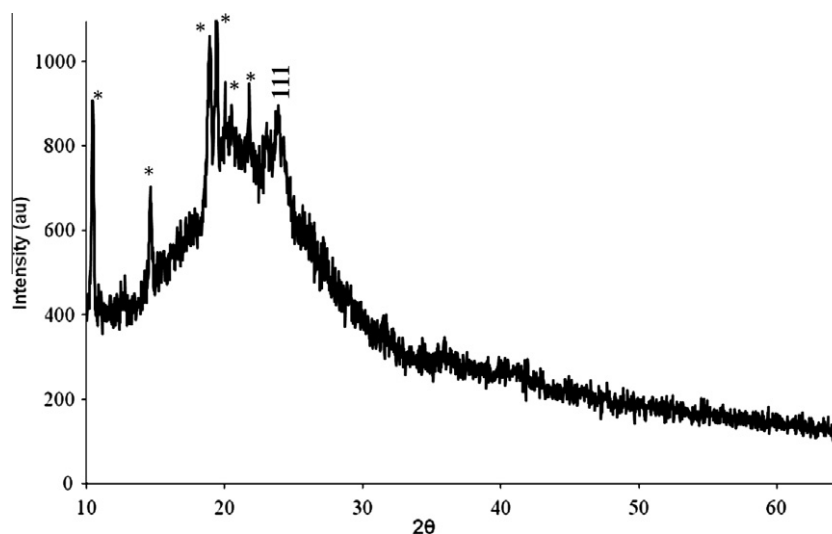


Fig. 9. XRD patterns of HDA-capped ZnS nanoparticles prepared from the zinc complex. (* – peaks due to the presence of hexadecylamine).

to the nature of bonding between the metal and the ligand through sulfur (M–S bond). The nanoparticles were prepared in a hot boiling solvent of hexadecylamine at a temperature of 120 °C, with HDA used for stabilizing nanoparticles. The complexes are generally air and thermally stable, such that their decomposition to yield metal sulfides took place at a temperature of 120 °C. Figs. 4–6 show

the TEM images of the HDA-capped CdS, HgS and ZnS nanoparticles, prepared from their corresponding complexes. HgS nanoparticles, under the synthetic conditions, produced spherical and oval shapes, with some intercalated, with sizes ranging from 8 to 25 nm and with a good uniform size distribution throughout the sample (Fig. 5). A single particle shows good crystalline features

with perfect alignment of the atoms. The zinc complex produced stacks of concentric ZnS particles, which are highly crystalline with concentric lattice planes (Fig. 6) and with particle sizes in the range 63–91 nm and d-lattice spacings of 2.27 nm. The powder X-ray diffraction patterns for the nanoparticles prepared from the complexes are shown in Figs. 7–9. ZnS nanoparticles show the predominant 1 1 1 plane of the cubic phase on their XRD pattern. The cadmium complex produced growth of particles in the hexagonal phase with XRD patterns indexed to 1 1 1, 2 0 0, 2 2 0, 3 1 1 and 4 0 0 for the peaks with 2θ values of 25.9, 29.5, 43.1 and 51.1, respectively. The peaks are broad, indicative of nanoscale particles. HgS nanoparticles gave crystalline particles with predominant peaks at 25.9, 29.5, 43.1 and 51.1 indexed to 1 1 1, 2 0 0, 2 2 0 and 3 1 1, respectively.

The complexes used to prepare these nanoparticles have similar ligand features, such as the alkyl group used – ethyl and methyl, and the corresponding phenyl substituent which influences the formation of needle-like, oval and concentric particles for the cadmium and mercury and the zinc complexes, respectively. Memon et al. [34] reported the synthesis of ZnS and CdS using bis(dodecyl)dithiocarbamate cadmium and zinc complexes, which produced rods and tetrapods at higher temperatures than 120 °C used in this work, while the morphologies are similar with different particles sizes.

4. Conclusion

Zn(II), Cd(II) and Hg(II) complexes of N,N-methyl phenyl-N,N-ethyl phenyl dithiocarbamate complexes have been prepared and characterized by elemental analyses and spectroscopic techniques. Four coordinate geometries are proposed for the complexes. The complexes were used as a single source precursor to synthesise ZnS, CdS and HgS semiconductor nanoparticles. The nanoparticles showed a blue shift in their absorption band edges, and emissions which are red shifted. The alkyl and phenyl substituents appear to influence the overall shape of the particles. The mercury complex was effective as a precursor to produce particles of uniform size that are highly crystalline, hexagonal and cubic phases with one predominant 1 1 1 plane, driven by hexadecylamine.

Acknowledgements

The authors are grateful to GMRDC, University of Fort Hare, South Africa for financial support and the University of Witwatersrand for providing space for the preparation of the nanoparticles. Special mention goes to Mr. Siya Mpelane who helped with the

XRD, TEM and HRTEM images from the CSIR, NCNSM, 1-Meiring Naude, Brummeria, 0001.

References

- [1] L.I. Victoriano, *Polyhedron* 19 (2000) 2269.
- [2] S. Thirumaran, V. Venkatachalam, A. Manohar, K. Ramalingam, G. Bocelli, A. Cantoni, *J. Coord. Chem.* 44 (1998) 281.
- [3] J. Stary, K. Kratzer, *J. Radioanal. Nucl. Chem. Lett.* 165 (1992) 137.
- [4] Y.E. Pazukhina, N.V. Isakova, V. Nagy, O.M. Petrukhin, *Solvent Extr. Ion Exch.* 15 (1997) 777.
- [5] L. Monser, N. Adhoum, *Sep. Purif. Technol.* 26 (2002) 137.
- [6] E.I. Stiefel, K. Matsumoto, in: *Transition Metal Sulfur Chemistry ACS Symposium Series*, vol. 653, American Chemical Society, Washington, DC, 1995, p. 2.
- [7] F. Caruso, M.L. Chan, M. Rossi, *Inorg. Chem.* 36 (1997) 3609.
- [8] D. Coucouvanis, *Prog. Inorg. Chem.* 26 (1979) 301.
- [9] G. Hogarth, *Prog. Inorg. Chem.* 53 (2005) 71.
- [10] J.J. Steggerda, J.A. Cras, J. Willemse, *Rec. Trav. Chim.* 100 (1981) 41.
- [11] D.P. Dutta, V.K. Jain, A. Knoedler, W. Kaim, *Polyhedron* 21 (2002) 239.
- [12] N. Srinivasan, P. Jamuna Rani, S. Thirumaran, *J. Coord. Chem.* 62 (2009) 1271.
- [13] D. Fan, M. Afzaal, M.A. Malik, C.Q. Nguyen, P. O'Brien, P.J. Thomas, *Coord. Chem. Rev.* 251 (2007) 1878.
- [14] R. Romano, O.L. Alves, *Mater. Res. Bull.* 41 (2006) 376.
- [15] R.D. Pike, H. Cui, R. Kershaw, K. Dwight, A. Wold, T.N. Blanton, A.A. Wernberg, H.J. Gysling, *Thin Solid Films* 224 (1993) 221.
- [16] T. Trindade, P. O'Brien, Xiao-mei Zhang, *Chem. Mater.* 9 (1997) 523.
- [17] M. Green, P. O'Brien, *Adv. Mater. Opt. Electron.* 7 (1997) 277.
- [18] B. Ludolph, M.A. Malik, P. O'Brien, N. Revaprasadu, *Chem. Commun.* (1998) 1849.
- [19] N.L. Pickett, P. O'Brien, *Chem. Rec.* 1 (2001) 467.
- [20] M. Green, P. Prince, M. Gardener, J. Steed, *Adv. Mater.* 16 (2004) 994.
- [21] N. Manav, A.K. Mishra, N.K. Kaushik, *Spectrochim. Acta A* 65 (2006) 33.
- [22] Thirumram, K. Ramalingam, G. Bocelli, A. Cantoni, *Polyhedron* 19 (2000) 1279.
- [23] M. Bonamico, G. Mazzone, A. Vaciago, I. Zambonelli, *Acta Crystallogr.* 19 (1965) 898.
- [24] S.K. Jha, B.H.S. Thimmappa, P. Mathur, *Polyhedron* 5 (1986) 2123.
- [25] S.A.A. Nami, K.S. Siddiqi, *Synth. React. Inorg., Met.-Org. Chem.* 34 (2004) 1583.
- [26] B.W. Wenclawiak, S. Uttich, H.J. Deiseroth, D. Schmitz, *Inorg. Chim. Acta* 3 (2003) 348.
- [27] L. Ronconi, L. Giovagnini, C. Marzano, F. Bettio, R. Graziani, G. Pilloni, D. Fregona, *Inorg. Chem.* 44 (2005) 1874.
- [28] M. Sarwar, S. Ahmad, S. Ahmad, S. Ali, S.A. Awan, *Transition Met. Chem.* 32 (2007) 200.
- [29] F. Bensebaa, Y. Zhou, A.G. Brolo, D.E. Irish, Y. Deslandes, E. Kruus, T.H. Ellis, *Spectrochim. Acta A* 55 (1999) 1229.
- [30] B.A. Prakasam, K. Ramalingam, G. Bocelli, A. Cantoni, *Polyhedron* 26 (2007) 4491.
- [31] G. Hogarth, C. Ebony-Jewel, R.C.R. Rainford-Brent, S.E. Kabir, I. Richards, J.D.E.T. Wilton-Ely, Q. Zhang, *Inorg. Chim. Acta* 362 (2009) 2021.
- [32] N. Srinivasan, S. Thirumaran, S. Ciattini, *J. Mol. Struct.* 938 (2009) 234.
- [33] S.P. Sovilj, G. Vukovi, K. Babic, T.J. Sabo, S. Macura, N. Juranic, *J. Coord. Chem.* 41 (1997) 25.
- [34] R.J. Anderson, D.J. Bendell, P.W. Groundwater, *Organic Spectroscopic Analysis*, RSC, Cambridge, 2004, p. 91.
- [35] M. Grenier-Loustalot, L. Da Cunha, *Eur. Polym. J.* 34 (1998) 98.
- [36] A.A. Memon, M. Afzaal, M.A. Malik, C.Q. Nguyen, P. O'Brien, *J. Chem. Soc., Dalton Trans.* (2006) 4499.
- [37] T. Mthethwa, S.R.R. Pullabhotla, P.S. Mdluli, J. Wesley-Smith, N. Revaprasadu, *Polyhedron* 9 (2009) 2977.